designs

Review

Inertial Measurement Units (IMUs) in Mobile Robots over the Last Five Years: A Review

Gerasimos G. Samatas [1] and Theodore P. Pachidis [2,*]

[1] MLV Research Group, Computer Science Department, International Hellenic University, 65404 Kavala, Greece; gesamat@cs.ihu.gr
[2] Human–Machines Interaction (Humain) Lab, Computer Science Department, International Hellenic University, 65404 Kavala, Greece
* Correspondence: pated@cs.ihu.gr; Tel.: +30-2510-462281

Abstract: Robots and especially mobile robots have experienced rapid growth, making them part of everyday life. An inertial measurement unit (IMU), which is a set of sensors, plays an important role in mobile robots' navigation. Data collected by the IMU sensors on a robot are properly converted and useful information is calculated concerning, i.e., position, orientation, and acceleration. With the advancement of technology, IMUs have been transformed from large and complex devices into small, flexible, and efficient ones. The main sensors included in an IMU are the gyroscope, the accelerometer, and the magnetometer. Additionally, there are other sensors such as a barometer, a temperature sensor, a pressure sensor, or even an attitude sensor. The components that an IMU consists of are many and the main differences concern the technology they integrate, the designer purpose, and the specifications set by the manufacturer. The purpose of this review is a comparative presentation of 42 IMU models from 7 different manufacturers over the last five years comparing main features such as structure details, connectivity, and communication protocols. Moreover, statistical results are quantitatively and qualitatively presented providing a future user the possibility to select the proper IMU.

Keywords: mobile robots; commercial Inertial Measurement Unit (IMU); sensors

Citation: Samatas, G.G.; Pachidis, T.P. Inertial Measurement Units (IMUs) in Mobile Robots over the Last Five Years: A Review. *Designs* **2022**, *6*, 17. https://doi.org/10.3390/designs6010017

Academic Editor: Oscar Reinoso Garcia

Received: 19 January 2022
Accepted: 14 February 2022
Published: 16 February 2022

1. Introduction

Nowadays, the word robot is very familiar to people. A major category of robots is mobile robots. Mobile robots can navigate using various sensors, software, properly developed and intelligent algorithms. Robots navigation is a complex process and to achieve it, many challenges must be overcome.

For the successful navigation of a robot, many open problems exist. These problems concern localization, mapping, simultaneous localization and mapping, path planning, obstacle avoidance. For localization, different sensors and methods have been developed for more accurate positioning [1]. There are different techniques for calculating the robot location, in a relative or absolute way. Techniques that calculate robot location in an absolute way are based on widespread systems. One well-known example is the Global Position System (GPS), which determines the current position with the assistance of satellites [2]. Techniques that relatively calculate robot location take into account previous states using various sensors such as the Inertial Measurement Unit (IMU) [3].

An IMU is an electronic device based on a set of sensors that takes into account data generated by them. Basic sensors are accelerometers, gyroscopes, or even magnetometers. The data generated—depending on the type of IMU—concern acceleration, angular velocity, as well as orientation in three directions respectively. Each sensor takes into account a reference axis making it mandatory to have one sensor for each lateral, longitudinal, and vertical axis for each accelerometer, gyroscope, and magnetometer, part of the device. Thus, there is a total output of nine different parameters (9 DOF) [4].

Historically, inertial measurement units have made evolutionary leaps after many years of research. Based on the acquisition method of the data, their development is divided into three stages. At first, there are the mechanical gyroscopes from 1940 to 1960, then the strap down gyroscopes (placed along with the object) with a time frame from 1960 to 1980. From 1980 until today there are the micro electro-mechanical gyroscopes. The transition to micro electro-mechanical technologies was considered very important, as they moved from large and expensive gyroscopes to devices smaller in size, less weight, and reduced cost while increasing their reliability. Along with the gyroscopes, small accelerometers and magnetometers have been also created and today they are manufactured very small, reliable, and cost-effective IMUs known as Micro Electro Mechanical Systems (MEMS) [5].

This paper presents a comparative review on IMUs in the past five years and describes the models, features, structure, connectivity, and their communication protocols. Moreover, deploys comparative presentation on commercial IMU products and presents usage statistics on commercial and research mobile robots. The novelty of this work is to provide easy access to the list of 42 IMU products, with the above characteristics, for future commercial or research projects with them.

The next section refers to the literature review and in particular presents the literature selection protocol and the way the research was executed. The third one refers to the description of the selected models. More specific presents the 7 different manufacturers and two Tables (Tables 1 and 2) with features of 42 IMUs. The comparative presentation of model's features and the related analysis takes place at the fourth section. The fifth section provides the mobile robots usage statistics. Finally, at last section, the conclusions of this work are presented.

2. Literature Report

Literature report is a scientific method, widely used to review various topics of interest. It is secondary research, as it takes into account other scientific researches related to the same subject. After collecting the data, their evaluation follows and finally, we end up with the analysis in a documented way [6].

2.1. Bibliography Selection Protocol

- Research Question
  Q1: What are the IMU models used in the last 5 years?
  Q2: What are the properties, main features, structure, response speed, connectivity and protocols of IMUs over the last 5 years?
  Q3: What are the comparative differences in their characteristics?
  Q4: What are the most used IMUs?
- Research Database

To extract data necessary, the research was done in many databases from the Google Scholar website which has 90% of the scientific publications written in English [7]. Harzing's Publish or Perish (HPP) (http://www.harzing.com (accessed on 13 November 2020)) program was used to group the data and export it in processable form.

- Rejection Criteria

The following criteria were set, with criterion S1 occurring during the execution of the research.

K1: Publications must be written between the year 2016 and 2020 i.e., the last five years.
K2: Citations per year must be more than 4.
K3: Citations must be over 20.

- Quality Criterion
  K4: The publication should refer to mobile robots.
- Acceptance Criterion
  K5: Publications should refer the company or IMU model used in their research.

- Special Criterion
  S1: After the K1 through K5 application the number of publications per publisher should be at least 2.

2.2. Research Execution

Based on the above criteria and questions a query was designed in the HPP database. A time period from 2016 to 2020 was chosen. The title should include the word "Robot". With this title, robots are secured as the core element of the experiment. Then the keywords selected were: (IMU OR Inertial Measurement Unit) AND Mobile Robot. With the OR we ensure that no matter how the word is abbreviated or paraphrased it will appear. With AND we make it mandatory for the publication to be in the realm of mobile robots.

The execution of the above conditions in HPP took place on 13 November 2020, with a limit of 1000 results. At the end of the search, the data was integrated into a worksheet, and filters were applied to group them. In total we had 995 publications so K2 was implemented and 263 publications emerged. The average of references in the total data was 20.7, so K3 was applied and resulted in 65 publications. These were analyzed to apply the K5 criterion. There has been a phenomenon of some publications using the IMU to cite it as material but avoiding specifying the model. This resulted in 50 publications and 23 different IMU manufacturers. Therefore, it was deemed appropriate to include the S1 criterion so that the number of publications is at least 2. The final results of 36 publications are presented in Figure 1. Lastly, after applying the above-mentioned criteria the research showed the 7 IMU manufacturers that were mentioned the most in the last five years. Then the models of each manufacturer were researched from its website and any model that had at least one reference to a publication from 2016 to 2020 were analyzed in Tables 1 and 2 with their features. The final outcome was 42 models that have been used in recent years in mobile robots by the 7 selected manufacturers.

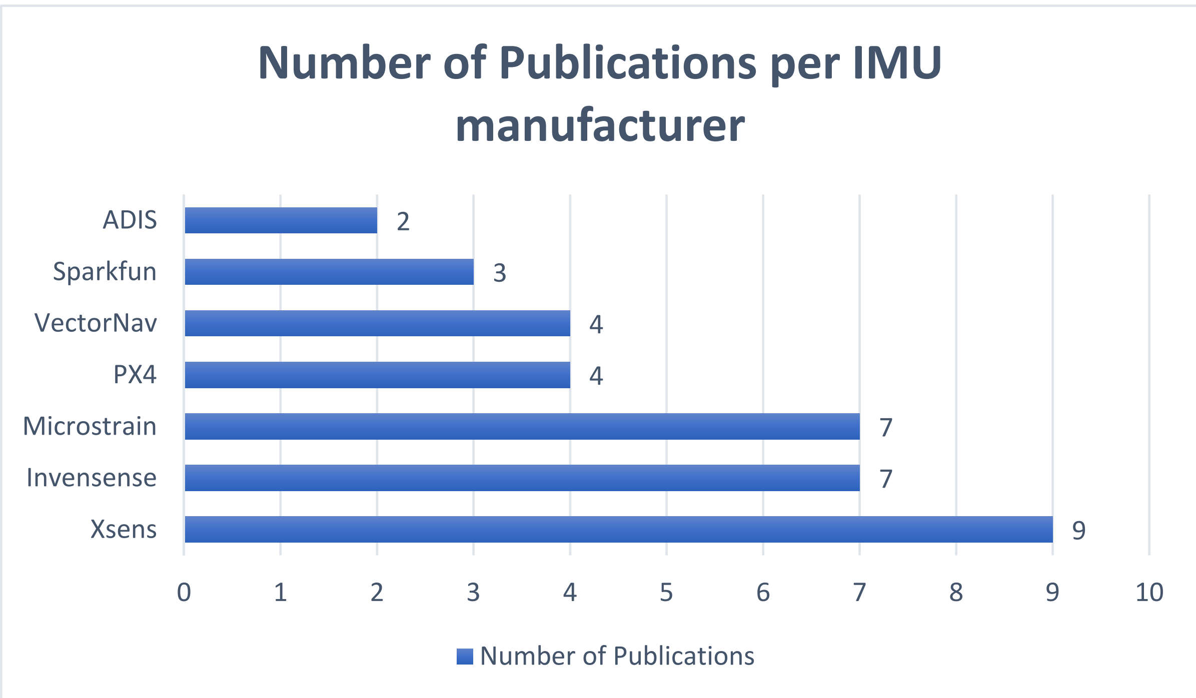

Figure 1. Publications per IMU manufacturer.

Table 1. Features of IMU's models. (1/2) ([Gyr] = Gyroscope, [Acc] = Accelerometer, [Mag] = Magnetometer, [Bar] = Barometer, [TS] = Temperature Sensor, [PS] = Pressure Sensor, [AS] = Attitude Sensor.]).

Manufacturer	Model	Voltage	Output Data Rate (HZ)	Gyroscope Range (°/s)	Accelerometer Range (g)	Magnetometer Range (G)	Power Consumption (mW)	Structure
Xsens	Mti-1	2.19–3.6	≤2000	±2000	±16	-	<100	Gyr, Acc,
	Mti-10	4.5–3.4	≤2000	±450	±20	±8	400–550	Gyr, Acc, Mag
	Mti-100	4.5–3.4	≤2000	±450	±20	±8	450–950	Gyr, Acc, Mag
	Mti-600	4.5–24	400–2000	±450	±20	±8	450–950	Gyr, Acc, Mag, Bar
InvenSense	MPU-9150	2.4–3.5	8000	±250, ±500, ±1000, ±2000	±2, ±4, ±8, ±16	±12	0.24–0.35	Gyr, Acc, Mag
	MPU-9250	2.4–3.5	8000	±250, ±500, ±1000, ±2000	±2, ±4, ±8, ±16	±48	1.8–2.62	Gyr, Acc, Mag
	MPU-6050	2.4–3.5	1000	±250, ±500, ±1000, ±2000	±2, ±4, ±8, ±16	-	9.5–13	Gyr, Acc
	ICM-20948	1.71–1.95	9000	±250, ±500, ±1000, ±2000	±2, ±4, ±8, ±16	±49	2.5	Gyr, Acc, Mag
	ICM-42605	1.7–3.6	8000	±125, ±250, ±500, ±1000, ±2000	±2, ±4, ±8, ±16	-	1.1–2.3	Gyr, Acc
	ICM-20602	1.7–3.6	8000	±250, ±500, ±1000, ±2000	±2, ±4, ±8, ±16	-	1.1–2.3	Gyr, Acc
	ITG-3050	2.1–3.6	-	±250, ±500, ±1000, ±2000	-	-	12.4–21.2	Gyr
	ITG-3200	2.1–3.6	8000	±2000	-	-	13.65–23.4	Gyr
	MPU-3050	2.1–3.6	3.9–8000	±250, ±500, ±1000, ±2000	-	-	13	Gyr
	MPU-3300	2.37–3.46	3.9–8000	±225, ±450	-	-	13	Gyr
	ICM-20608-G	1.71–3.45	4–8000	±250, ±500, ±1000, ±2000	±2, ±4, ±8, ±16	-	-	Gyr, Acc
Microstrain	3DM-GX5-10	4–36	1–1000	±75, ±150, ±300, ±900	±2, ±4, ±8, ±20, ± 40	-	300	Gyr, Acc, TS
	3DM-CX5-10	3.2–5.2	1–1000	±75, ±150, ±300 ±900	±2, ±4, ±8, ±20, ±40	-	300	Gyr, Acc, TS
	3DM-CV5-10	3.2–5.2	1–1000	±250, ±500, ±1000	±2, ±4, ±8	-	360	Gyr, Acc, TS
Pixhawk	Pixhawk 4	4.75–5.2	-	±250, ±500, ±1000, ±2000	±2, ±4, ±8, ±16	±16 (x,y), 25y	360	Gyr, Acc, Mag
	Pixhawk 3 Pro	3.3	-	±250, ±500, ±1000, ±2000	±2, ±4, ±8, ±16	±4, ±8, ±12, ±16	825	Gyr, Acc, Mag, Bar
	Pixracer	-	-	±250, ±500, ±1000, ±2000	±2, ±4, ±8, ±16	±8	-	Gyr, Acc, Mag, Bar
	Pixhawk	-	-	±245, ±500, ±2000	±2, ±4, ±8, ±16	±2, ±4, ±8, ±12	-	Gyr, Acc, Mag, Bar
ADIS	ADIS16475	3–3.6	2000	±125, ±450, ±2000	±8	-	132–158	Gyr, Acc
	ADIS16495	3–3.6	4500	±125, ±500, ±2000	±8	-	267–320	Gyr, Acc
	ADIS16465	3–3.6	2000	±125, ±500, ±2000	±8	-	450–950	Gyr, Acc
	ADIS16490	3–3.6	4250	±100	±8	-	267–320	Gyr, Acc
	ADIS16488	3.15–3.45	819	±450	±18	±2.5	240–262	Gyr, Acc, Mag, Bar
	ADIS16445	3.15–3.45	820	±62, ±125, ±250	±5	-	1.8–2.62	Gyr, Acc, Mag, Bar
	ADIS16448	3.15–3.45	819	±250, ±500, ±1000	±18	±1.9	239–262	Gyr, Acc, Mag, Bar
	ADIS16480	3–3.6	2460	±450	±10	±2.5	841	Gyr, Acc, Mag, PS
	ADIS16485	3–3.6	2460	±450	±5	-	650	Gyr, Acc
	ADIS16362	4.75–5.25	819.2	±75, ±150 ±300	±1.7	-	245	Gyr, Acc
	ADIS16365	4.75–5.25	819.2	±75, ±150 ±300	±18	-	120	Gyr, Acc

Table 1. *Cont.*

Manufacturer	Model	Voltage	Output Data Rate (HZ)	Gyroscope Range (°/s)	Accelerometer Range (g)	Magnetometer Range (G)	Power Consumption (mW)	Structure
SparkFun	VR IMU Breakout—BNO080	1.65–3.6	-	±2000	±8	-	45	Gyr, Acc, Mag
	IMU Breakout—LSM9DS1	3.3	-	±245, ±500, ±2000	±2, ±4, ±8, ±16	±4, ±8, ±12, ±16	14.85	Gyr, Acc, Mag
	SparkFun MPU-6050	2.4–3.5	1000	±250, ±500, ±1000, ±2000	±2, ±4, ±8, ±16	-	9.5–13	Gyr, Acc
	ESP32 Thing Motion Shield	3.3	80	±245, ±500, ±2000	±2, ±4, ±8, ±16	±4, ±8, ±12, ±16	13.2	Gyr, Acc, Mag
	SparkFun LSM6DS3	1.71–3.6	1600	±125, ±245, ±500, ±1000, ±2000	±2, ±4, ±8, ±16	±2, ±4, ±8, ±12, ±16	2.1–4.5	Gyr, Acc
VectorNav	VN-100	3.2–3.5 (WOC) 12–34 (WC)	800	±2000	±16	±2.5	185 (WOC), 200 (WC)	Gyr, Acc, Mag, PS
	VN-110	3.2–3.5 (WOC) 12–34 (WC)	800	±490	±15	±2.5	<1000 (WOC), <2000 (WC)	Gyr, Acc, Mag, PS, AS
	VN-200	3.2–5.5 (WOC) 3.3–17 (WC)	800	±2000	±16	-	445 (WOC), 500 (WC)	Gyr, Acc, PS
	VN-300	3.2–5.5 (WOC) 3.3–14 (WC)	400	±2000	±16	±2.5	<1250 (WOC), 1250 (WC)	Gyr, Acc, PS

Table 2. Features of IMU's models (2/2).

Manufacturer	Model	Gyroscope (Nonlinearity, Sensitivity, Noise Density)	Accelerometer (Nonlinearity, Sensitivity, Noise Density)	Weight (g)	Dimensions (mm)	Connectivity Protocols	Software	Cost (€)
Xsens	Mti-1	±0.1% fs, 0.001°/s/g, 0.007°/s/$\sqrt{\text{Hz}}$	±0.5% fs, -, 0.12 mg/$\sqrt{\text{Hz}}$	<1	12.1 × 12.1 × 2.55	I^2C, SPI, UART, Xbus	MT Software Suite	135
	Mti-10	±0.03% fs, 0.006°/s/g, 0.03°/s/$\sqrt{\text{Hz}}$	±0.1% fs, -, 0.06 mg/$\sqrt{\text{Hz}}$	11 (WOC) 52 (WC)	37 × 33 × 12 (WOC) 57 × 42 × 23.5 (WC)	RS232, RS485, RS422, UART, USB, Xbus		800
	Mti-100	±0.01% fs, 0.003°/s/g, 0.01°/s/$\sqrt{\text{Hz}}$	±0.1% fs, -, 0.06 mg/$\sqrt{\text{Hz}}$	11 (WOC) 52 (WC)	37 × 33 × 12 (WOC) 57 × 42 × 23.5 (WC)	RS232, RS485, RS422, UART, USB, Xbus		1470
	Mti-600	±0.1% fs, 0.001°/s/g, 0.007°/s/$\sqrt{\text{Hz}}$	±0.1% fs, -, 0.06 mg/$\sqrt{\text{Hz}}$	11 (WOC) 52 (WC)	37 × 33 × 12 (WOC) 57 × 42 × 23.5 (WC)	CAN, RS232, UART, Xbus		450

Table 2. *Cont.*

Manufacturer	Model	Gyroscope (Nonlinearity, Sensitivity, Noise Density)	Accelerometer (Nonlinearity, Sensitivity, Noise Density)	Weight (g)	Dimensions (mm)	Connectivity Protocols	Software	Cost (€)
InvenSense	MPU-9150	±0.2% fs, 0.0076°/s/LSB, 0.005°/s/√Hz	±0.5% fs, 0.061 mg/LSB, 0.4 mg/√Hz	-	4 × 4 × 1	I^{2}C	SmartRobotics	17
	MPU-9250	±0.1% fs, 0.0076°/s/LSB, 0.01°/s/√Hz	±0.5% fs, 0.061 mg/LSB, 0.3 mg/√Hz	-	3 × 3 × 1	I^{2}C, SPI		11.5
	MPU-6050	±0.2% fs, 0.0076°/s/LSB, 0.005°/s/√Hz	±0.5% fs, 0.061 mg/LSB, 0.4 mg/√Hz	-	4 × 4 × 0.9	I^{2}C		5
	ICM-20948	±0.1% fs, 0.0076°/s/LSB, 0.015°/s/√Hz	±0.5% fs, 0.061 mg/LSB, 0.23 mg/√Hz	-	3 × 3 × 1	I^{2}C, SPI		13.5
	ICM-42605	±0.1% fs, 0.061°/s/LSB, 0.0038°/s/√Hz	±0.1% fs, 0.488 mg/LSB, 0.07 mg/√Hz	-	2.5 × 3 × 0.91	I^{2}C, SPI		6
	ICM-20602	±0.1% fs, 0.0076°/s/LSB, 0.004°/s/√Hz	±0.3% fs, 0.061 mg/LSB, 0.1 mg/√Hz	-	3 × 3 × 0.75	I^{2}C, SPI		5
	ITG-3050	±0.2% fs, 0.0076 °/s/LSB, 0.001 °/s /√Hz	-	-	4 × 4 × 0.9	I^{2}C		2.5
	ITG-3200	±0.1% fs, 6.95 × 10^{-5}°/s/LSB, 0.003°/s/√Hz	-	-	4 × 4 × 0.9	I^{2}C		10.5
	MPU-3050	±0.2% fs, 0.0076°/s/LSB, 0.01°/s/√Hz	-	-	4 × 4 × 0.9	I^{2}C		7
	MPU-3300	±0.2% fs, 0.0068°/s/LSB, 0.005°/s/√Hz	-	-	4 × 4 × 0.9	I^{2}C, SPI		35
	ICM-20608-G	±0.1% fs, 0.0076°/s/LSB, 0.008°/s/√Hz	±0.5% fs, 0.061 mg/LSB, 0.25 mg/√Hz	-	3 × 3 × 0.75	I^{2}C, SPI		6.5
Microstrain	3DM-GX5-10	±0.02% fs, -, 0.005°/s /√Hz	±0.02% fs, -, 0.02 mg/√Hz	16.5	36 × 36.6 × 11	RS232, LXRS Protocol	SensorConnect	710
	3DM-CX5-10	±0.02% fs, -, 0.005°/s/√Hz	±0.02% fs, -, 0.02 mg/√Hz	8	38 × 24 × 9.7	RS232, LXRS Protocol		710
	3DM-CV5-10	±0.06% fs, -, 0.0075°/s/√Hz	±0.04% fs, -, 0.1 mg/√Hz	11	38 × 24 × 9.7	TTL serial, LXRS Protocol		710
Pixhawk	Pixhawk 4	±0.1% fs, 0.0076°/s/LSB, 0.006°/s/√Hz	±0.5% fs, 0.61 mg/LSB, 0.15 mg/√Hz	15.8	44 × 84 × 12	PWM, SBUS, I^{2}C, SPI, CAN	Open Source Autopilot	230
	Pixhawk 3 Pro	±0.1% fs, 0.0076°/s/LSB, 0.004°/s /√Hz	±0.3% fs, 0.061 mg/LSB, 0.1 mg/√Hz	45	71 × 49 × 23	PWM, SBUS, I^{2}C, SPI, SUMD, PPM		260
	Pixracer	±0.1% fs, 0.0076°/s/LSB, 0.008°/s/√Hz	±0.5% fs, 0.061 mg/LSB, 0.25 mg/√Hz	10.5	36 × 36	UART, USB, PWM, SBUS, I^{2}C, SPI, JTAG, PPM, ST24		265
	Pixhawk	±0.2% fs, 0.0076°/s/LSB, 0.005°/s/√Hz	±0.5% fs, 0.061 mg/LSB, 0.4 mg/√Hz	38	50 × 15.5 × 81.5	UART, PWM, SBUS, I^{2}C, SPI, PPM, USB, ST24, SUMD		230

Table 2. *Cont.*

Manufacturer	Model	Gyroscope (Nonlinearity, Sensitivity, Noise Density)	Accelerometer (Nonlinearity, Sensitivity, Noise Density)	Weight (g)	Dimensions (mm)	Connectivity Protocols	Software	Cost (€)
Analog Devises	ADIS16475	±0.2% fs, 0.00625°/s/LSB, 0.003°/s /$\sqrt{}$Hz rms	±0.25% fs, 3.8 × 10^{-6} mg/LSB, 0.023 mg/$\sqrt{}$Hz rms	1.3	11 × 15 × 11	SPI	CoolVision SDK	860
	ADIS16495	±0.2% fs, 9.53 × 10^{-8}°/s/LSB, 0.002°/s/$\sqrt{}$Hz rms	±0.25% fs, 3.8 × 10^{-6} mg/LSB, 0.017 mg/$\sqrt{}$Hz rms	42	47 × 44 × 14	SPI		2500
	ADIS16465	±0.2% fs, 0.00625°/s/LSB, 0.002°/s/$\sqrt{}$Hz rms	±0.25% fs, 3.8 × 10^{-6} mg/LSB, 0.023 mg/$\sqrt{}$Hz rms	-	22.4 × 22.4 × 9	SPI		630
	ADIS16490	±0.3% fs, 7.63 × 10^{-8}°/s/LSB, 0.002°/s/$\sqrt{}$Hz rms	±0.1% fs, 7.63 × 10^{-6} mg/LSB, 0.016 mg/$\sqrt{}$Hz rms	42	47 × 44 × 14	SPI		3170
	ADIS16488	±0.01% fs, 3.052 × 10^{-7}°/s/LSB, 0.0059°/s/$\sqrt{}$Hz rms	±0.1% fs, 1.221 × 10^{-5} mg/LSB, 0.063 mg/$\sqrt{}$Hz rms	-	24.1 × 37.7 × 10.8	SPI		1800
	ADIS16445	±0.1% fs, 0.01°/s/LSB, 0.011°/s/$\sqrt{}$Hz rms	±0.2% fs, 0.25 mg/LSB, 0.105 mg/$\sqrt{}$Hz rms	-	24.1 × 37.7 × 10.8	SPI		550
	ADIS16448	±0.1% fs, 0.04°/s/LSB, 0.0135°/s/$\sqrt{}$Hz rms	±0.2% fs, 0.833 mg/LSB, 0.23 mg/$\sqrt{}$Hz rms	-	24.1 × 37.7 × 10.8	SPI		650
	ADIS16480	±0.01% fs, 3.052 × 10^{-7}°/s/LSB, 0.0066°/s/$\sqrt{}$Hz rms	±0.1% fs, 1.221x10^{-6} mg/LSB, 0.067 mg/$\sqrt{}$Hz rms	48	47 × 44 × 14	SPI		2960
	ADIS16485	±0.01% fs, 3.052 × 10^{-7}°/s/LSB, 0.0066°/s/$\sqrt{}$Hz rms	±0.1% fs, 3.815x10^{-5} mg/LSB, 0.055 mg/$\sqrt{}$Hz rms	48	47 × 44 × 14	SPI		1600
	ADIS16362	±0.1% fs, 0.05°/s/LSB, 0.044°/s/$\sqrt{}$Hz rms	±0.1% fs, 0.333 mg/LSB, 0.23 mg/$\sqrt{}$Hz rms	16	23 × 23 × 23	SPI		460
	ADIS16365	±0.1% fs, 0.05°/s/LSB, 0.044°/s/$\sqrt{}$Hz rms	±0.1% fs, 0.333 mg/LSB, 0.5 mg/$\sqrt{}$Hz rms	16	23 × 23 × 23	SPI		605
SparkFun	VR IMU Breakout—BNO080	±0.05% fs, 0.0625°/s/LSB, -	±0.5% fs, 1 mg/LSB, 0.19 mg/$\sqrt{}$Hz	-	26 × 31.2	UART, I^2C, SPI, SHTP	Arduino IDE	30
	IMU Breakout—LSM9DS1	-, 0.00875 °/s/LSB, -	-, 0.061 mg/LSB, -	-	23 × 23	UART, I^2C, SPI, SHTP		14
	SparkFun MPU-6050	±0.2% fs, 0.0076°/s/LSB, 0.005°/s/$\sqrt{}$Hz	±0.5% fs, 0.061 mg/LSB, 0.4 mg/$\sqrt{}$Hz	-	25.5 × 15.2 × 2.48	I^2C		25
	ESP32 Thing Motion Shield	-, 0.00875°/s/LSB, -	-, 0.061 mg/LSB, -	-	-	SPI, I^2C, microSD		20
	SparkFun LSM6DS3	-, -, 0.007°/s/$\sqrt{}$Hz	-, 0.061 mg/LSB, 0.09 mg/$\sqrt{}$Hz	-	2.5 × 3 × 0.83	SPI, I^2C		10

Table 2. *Cont.*

Manufacturer	Model	Gyroscope (Nonlinearity, Sensitivity, Noise Density)	Accelerometer (Nonlinearity, Sensitivity, Noise Density)	Weight (g)	Dimensions (mm)	Connectivity Protocols	Software	Cost (€)
VectorNav	VN-100	-, -, 0.0035°/s/$\sqrt{\text{Hz}}$	-, -, 0.14 mg/$\sqrt{\text{Hz}}$ rms	3.5 (WOC) 15 (WC)	24 × 22 × 3 (WOC) 36 × 33 × 9(WC)	TTL serial, SPI (WOC), RS-232 (WC)	VectorNav Control Center	700
	VN-110	-, -, 0.0138°/s/$\sqrt{\text{Hz}}$	-, -, 0.04 mg/$\sqrt{\text{Hz}}$ rms	12 (WOC) 125 (WC)	31 × 31 × 11(WOC) 56 × 56 × 23(WC)	Serial TTL (WOC), RS-422 (WC)		-
	VN-200	-, -, 0.0035°/s/$\sqrt{\text{Hz}}$	-, -, 0.14 mg/$\sqrt{\text{Hz}}$ rms	4 (WOC) 16 (WC)	24 × 22 × 3(WOC) 36 × 33 × 9.5(WC)	TTL serial, SPI (WOC), RS-232 (WC)		2300
	VN-300	-, -, 0.0035°/s/$\sqrt{\text{Hz}}$	-, -, <0.14 mg/$\sqrt{\text{Hz}}$ rms	4 (WOC) 16 (WC)	24 × 22 × 3(WOC) 45 × 44 × 11(WC)	TTL serial, SPI (WOC), RS-232 (WC)		-

3. IMU Models Description

The result shows 7 different IMU manufacturers and 42 IMU models. This section has two parts. The first one is the description of the IMU manufacturers and the second is the two Tables with the entire models, features, structure, cost, connectivity, and their communication protocols grouped by manufacturer.

3.1. Manufacturers

The first company on the list was Xsens (https://www.xsens.com/ (accessed on 13 November 2020)) with 9 papers and 4 different models [8–16]. The company was founded in 2000 in The Netherlands and specializes in the creation of motion tracking sensors. For this technology, it has created its own IMU sensors. The next company was Invensense (https://invensense.tdk.com/ (accessed on 13 November 2020)) with 7 reports and 11 models respectively [17–23]. The company based in California was founded in 2003 and specializes in integrated circuits with integrated sensors. Microstrain (https://www.microstrain.com/ (accessed on 13 November 2020)) is the next manufacturer with 7 papers and 6 models [24–30]. The company was founded in the USA in 1987 and produces sensors for industry and research.

Furthermore, the Pixhawk (PX4) was the next manufacturer. It is an open-source system used primarily for flying robots as all its functions are geared towards them. The company doesn't manufacture IMUs but assembles components. PX4 had 4 publications and one model per publication 4 in total [31–34]. Fifth in order was VectorNav (https://www.vectornav.com/ (accessed on 13 November 2020)) with 4 publications and 4 models also [35–38]. The company was founded in 2008 in the USA and deals mainly with IMU systems for aerial robots. Next was Sparkfun (https://www.sparkfun.com/ (accessed on 13 November 2020)), a retail company founded in 2003 and based in the USA. It also manufactures, among other things, IMUs by integrating individual components from third parties and presented under the company name and has 3 references for 4 models [39–41]. The last company on the list was Analog Devices (ADIS) (https://www.analog.com/ (accessed on 13 November 2020)) with 2 publications [42,43]. Founded in 1965 and specializes in designing and manufacturing precision electronic equipment including IMUs. The models analyzed were 11 in total.

3.2. IMU Features Tables

This section contains IMUs with features (Tables 1 and 2) extracted from the official website of manufacturers described in Section 3.1. Table 1 includes the input voltage, output data rate, gyroscope—accelerometer—magnetometer range, power consumption, and structure. Table 2 includes three basic features (nonlinearity, sensitivity and noise density) of the two main sensors of each IMU (gyroscope and accelerometer). It includes also the weight, dimensions, connectivity protocols, supporting software, and cost of IMUs. The cost feature in Table 2 was calculated in € with fixed exchange rates (1€ = 0.84 £ = 1.12$). Also, response speed and operational temperature range were extracted but the importance of these features was low. At first, only 6 of the 42 models (14%) had response speed data. The Mti-series had the faster response speed (2 ms) and the SparkFun LSM9DS1 and BNO080 had the slower one (6.6 ms). The operating temperature had only two values, 30 models had operating temperature from −40 °C to +85 °C, which indicates that they are categorized as an industrial range. The ADIS (Analog Devises) models (11 in total) had from −40 °C to 105 °C. Furthermore, ADIS, because of the aforementioned difference at the maximum range (20 °C), has categorized their products as AEC-Q100 Level 2, which corresponds to a higher grade than the industrial range.

4. Features Comparative Presentation and Analysis

First feature examined was the input voltage. In case where there was a range of values, the average value was calculated to easily compare the results and in models with two case options (case and without case) the input voltage without a case was chosen. The Mti-10 and Mti-100 models had the highest input voltage, 21.5 Volts. The lower voltage, 2.6 Volts belongs to the ICM-20608-G and SparkFun VR IMU Breakout. The 77.5% of models had a voltage less than or equal to 5 Volts (Figure 2).

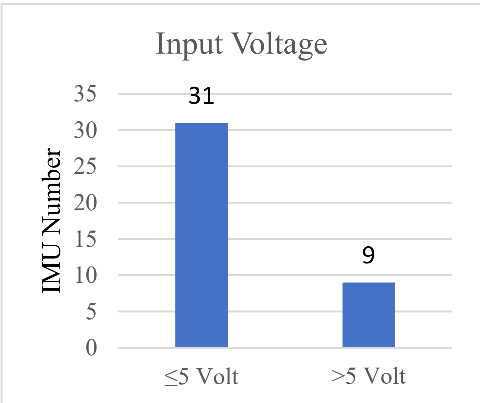

Figure 2. The input Voltage statistics divided in two classes.

Most of the models had output data rate below 8000 Hz (26 models, 72.2%). The ESP32 Thing Motion Shield model of SparkFun had the lower value at 80 Hz. Among the others, 9 models (25%), had exactly 8000 Hz. Finally, the ICM-20948 was the only one with 9000 Hz (Figure 3).

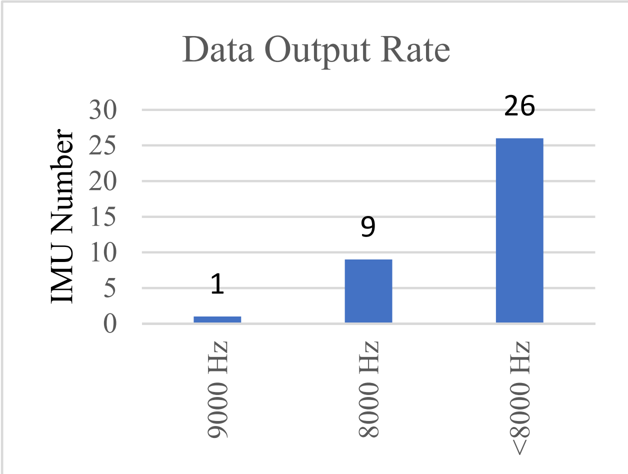

Figure 3. Data Output rate.

To compare the power consumption in mW, in some cases, values have been converted properly. Also, in cases with a range of values, the maximum value was selected. It is found that the highest consumption was 2000 mW of the Vn-110 model and the lowest one was 0.35 mW of MPU-9150.

The measurement range of sensors (gyroscope, accelerometer, and magnetometer) is properly selected according to the measurements required. Some models had more than one range of values. Unnecessary measurements create problems in data transmission. The gyroscope measures angular velocity in °/s (±). The lowest value was 15.625°/s (±) at the ICM-42605 model. The highest value was 2000°/s (±). The 62% of the IMUs examined had this value at their highest range. Also, 38% have at least 4 range options (Figure 4). The accelerometer measures acceleration in g (±) where g is the acceleration of gravity. The lowest value was 1.7 g at the ADIS16362 model, and the highest was 40 g at the 3DM-GX5-10 and 3DM-CX5-10 models. 50% of all models had the highest range value 16g and the lowest 2 g (Figure 5). Finally, the magnetometer's measurement unit is G (±) that is Gauss. Some of the data needed to be converted from μT to G. The lowest value was 1.9 G and belonged to the ADIS16448 model while the highest values were 49 G and corresponded to the ICM-20948 model. Also, 75% had up to 3 different ranges (Figure 6).

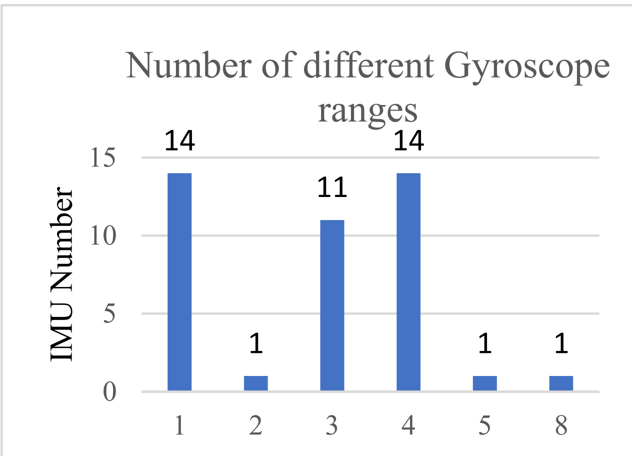

Figure 4. The different ranges of Gyroscopes.

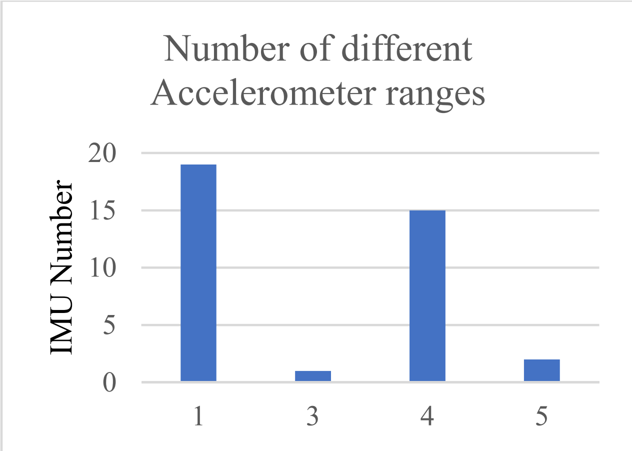

Figure 5. The different ranges of Accelerometers.

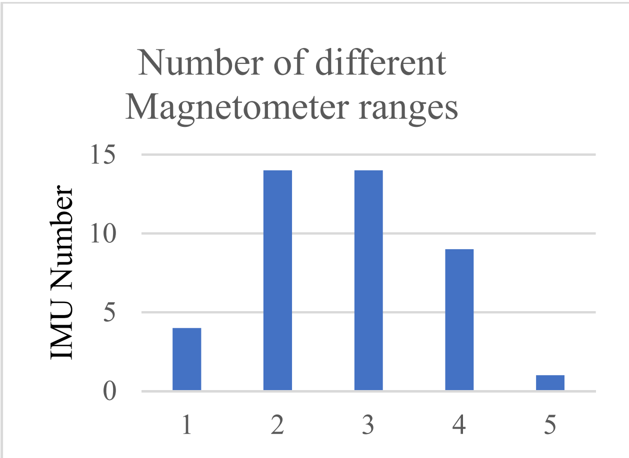

Figure 6. The different ranges of Magnetometers.

In Table 2 data from manufacturers' datasheets for nonlinearity, sensitivity, and noise density of the two main sensors of each IMU (gyroscope and accelerometer) are provided. Features as accuracy and resolution are not systematically provided in the manufacturers' datasheets. However, the accuracy is inversely proportional to the sensitivity and takes into account the measurement errors due to the noise. Sensors calibration is required to remove inaccuracies stemming from manufacturing imperfections. Sensors' resolution can be calculated from noise density for a specific bandwidth. The nonlinearity concerns the systematic deviation from the straight line that defines the nominal input-output relationship. It is typically expressed as a percentage of scale factor (% fs), where fs stand for full scale. The minimum value of $\pm$0.01% fs was found for Mti-100, ADIS16480, ADIS16485, and ADIS16488 IMUs, while the maximum one was $\pm$0.3% fs for ADIS16490 IMU. Sensitivity expresses the ratio of change in input to change in the output signal. Sensitivity units are typically expressed in $^\circ$/s/g and $^\circ$/s/LSB for gyroscopes and in mV/g for analog-output accelerometers, LSB/g, or mg/LSB for digital-output accelerometers. The minimum sensitivity values for gyroscopes, 0.001°/s/g, and 7.63×10^{-8} $^\circ$/s/LSB were found in Mti-1 and ADIS16490 IMUs respectively. The maximum sensitivity value has the Breakout—BNO080 IMU (0.0625°/s/LSB). For accelerometers, the range of sensitivity values was between 1.221×10^{-6} mg/LSB (ADIS16480 IMU), and 1 mg/LSB (Breakout—BNO080 IMU). The more common measure of noise is noise density (power spectral density) which provides the noise divided by the square root of the sampling rate. Noise density units are in $^\circ/s/\sqrt{Hz}$ or $^\circ/s/\sqrt{Hz}$ rms for gyroscopes, and in mg/$\sqrt{Hz}$ or mg/$\sqrt{Hz}$ rms for accelerometers. The range of noise density values for gyroscopes presented in Table 2 is from 0.002$^\circ/s/\sqrt{Hz}$ rms (ADIS16490, ADIS16495, and ADIS16465) to 0.044$^\circ/s/\sqrt{Hz}$

rms (ADIS16362, and ADIS16365). Minimum noise density values for accelerometers were 0.02 mg/$\sqrt{\text{Hz}}$ (3DM-GX5-10, 3DM-CX5-10), and 0.016 mg/$\sqrt{\text{Hz}}$ rms, for ADIS16490 IMUs. The maximum noise density is presented in ADIS16365 IMU (0.5 mg/$\sqrt{\text{Hz}}$ rms).

There are several communication protocols and connectivity methods referred to models specifications. In summary, different models may have some of the following protocol-connection methods: I^2C, SPI, UART, Xbus, RS232, RS485, RS422, USB, CAN, I3CSM, LXRS, TTL Serial, PWM, SBUS, Spectrum, SUMD, PPM, ST24, SHTP, microSD. The main protocols were I^2C and SPI with 83.33% of the models having at least one of them. The Pixhawk and Pixracer models have 9 different protocol-connection methods. The reason that they were listed together is because most of the times a communication protocol is the same as the connection method.

The next characteristic is structure and refers to different combinations of sensors in each IMU. The basic sensors are gyroscopes, magnetometers, and accelerometers. There are also IMUs with other sensors such as barometers, temperature, and altitude pressure sensors. The range of different number of IMU sensors varies from one to five. Figure 7 shows, how many IMUs belong to these five categories. All IMUs had a gyroscope. Even more, 90% of them had an accelerometer. 40% of them also had magnetometers. All IMUs that had a magnetometer had also an accelerometer and a gyroscope. The 38% had at least one barometer, pressure, temperature, or attitude sensor. More specifically, 43% were barometers, 31.3% were pressure sensors, 18.8% were temperature sensors and only one sensor was attitude sensor. (6.25%).

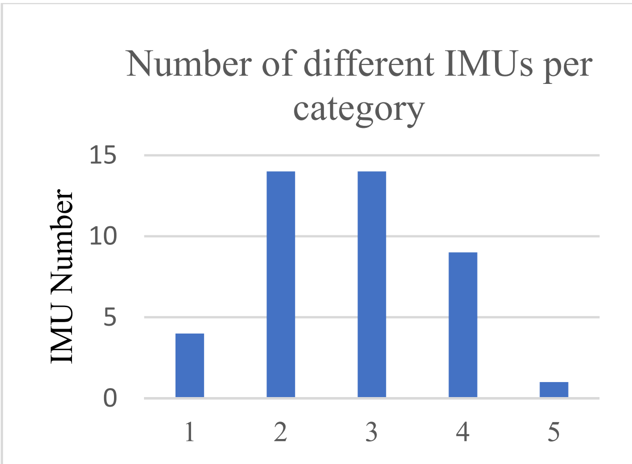

Figure 7. Number of IMUs depending on the number of sensors they include.

5. Usage Statistics

The following method was designed to derive usage statistics. Initially, the 7 most dominant companies were searched on the HPP platform, through the Google Scholar website, the times that they appear in total, with the following criteria: The search space of time remains from 2016 to 2020 and keywords are the "company name" AND "mobile Robot". In the company Analog Devices (ADIS), due to the common name, all the ADIS models of Table 1 were searched by their name. The overall results in descending order of use are presented in Figure 8, which displays the number of different IMU model applications from the 7 companies analyzed in the previous chapters. Xsens and Invensense are pioneers. They covered 47.19% of total applications.

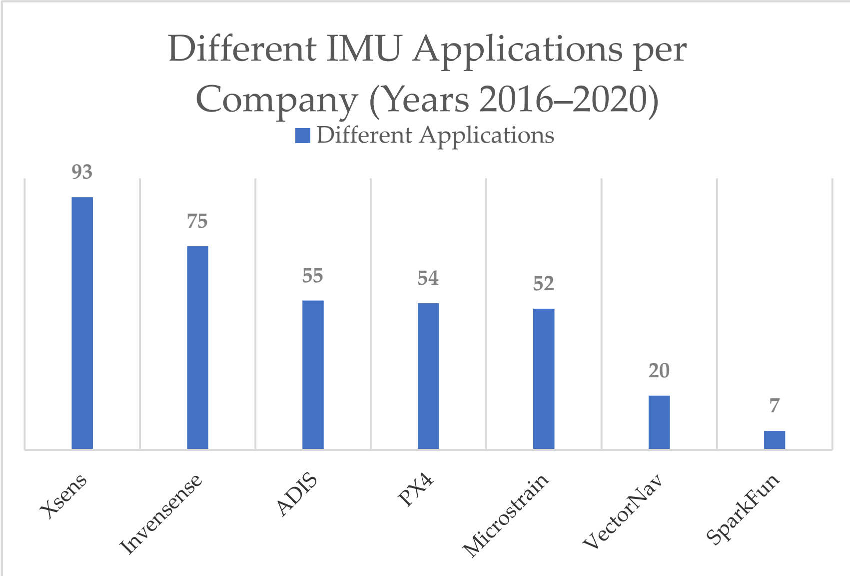

Figure 8. Total number of IMU applications per company in years 2016–2020.

Then there was ADIS, Pixhawk, and Microstrain with 55, 54, and 52 distinct applications respectively which corresponds to a total of 45%. Finally, there were Vector Nav and SparkFun with much smaller percentages, 5.62%, and 1.97% respectively. Also, Figure 9 shows the same data broken down by year to highlight the trend of each company and the usage trends of IMU companies per year. Bearing in mind in 2020 that, on one hand, the date on which the report was written was not nearly at the end of the year, and on the other hand, that in 2020 there is a health crisis with the COVID pandemic and all areas such as global research has been affected [44]. This can be seen also from Figure 9 that all companies from 2019 to 2020 showed a decline. In case, taking into account the year 2019, the companies Xsens, Invensense, Pixhawk, and ADIS had an upward trend, while Microstrain, VectorNav, and Sparkfun had a downward. The largest increase is presented by the company Xsens, which managed to surpass Invensense, which also had an increasing trend but at a slower pace.

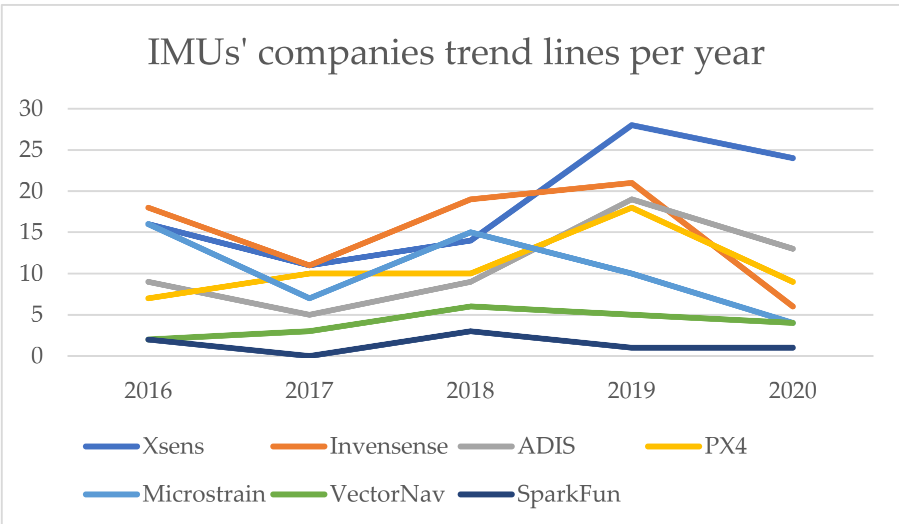

Figure 9. Trend lines of the 7 IMUs' companies in years 2016–2020.

6. Conclusions

The present review of different commercial IMUs, through a systematic way of research, refers to 42 IMU models. The number was obtained through a predefined method, described in previous sections, searching applications of the 7 manufacturers, which in turn emerged through research from 36 publications dealing with the construction of mobile robots in the last five years. Their selection through 995 publications was made through the criteria presented. Then, a detailed presentation in the form of a table of the main features, and data of each model was made. After that, the features were presented comparatively and analyzed. Also, usage statistics were presented through Figures 8 and 9. In some cases, the companies didn't have available information for some features. One such feature was the response time. Also, in some cases the measurement unit was different and as a result, the direct comparison of the features between models was not obvious, and conversion was needed. Conversely, the features were easily available to anyone interested.

During the feature comparison, the necessity of writing the present review was revealed, as there are several differences among the models. Most of the differences were significant and affected the outcome of making a mobile robot. Large or small range values do not mean better or worse sensors respectively. Thus, with the aggregate presentation of the data, the appropriate choice becomes easier. The choice must be made based on the data to be measured. There were also companies with an integrated IMU such as Pixhawk and companies that provided only the main sensor at the integrated circuit level. In terms of usage statistics, the years and companies surveyed showed a trend, with a clear upward and downward trend of the companies. An exception is the year 2020, which, as mentioned, due to the COVID-19 pandemic, had a universal downward trend.

The selection criteria of the publications and the models are also mentioned in detail so that in the future the interested researcher can configure them and be led to additional companies with more models for further analysis. Even the features presented are specific, forming a small part of the whole of them and in the future, other major features could be examined and as a result, different comparatives tables could be created.

Finally, the future design of a prototype feature framework is proposed depending on the use of IMU in order to be more efficient in comparing the different models.

Author Contributions: Writing—review and editing, G.G.S. and T.P.P. All authors have read and agreed to the published version of the manuscript.

Funding: This research received no external funding.

Institutional Review Board Statement: Not applicable.

Informed Consent Statement: Not applicable.

Data Availability Statement: Not applicable, the study does not report any data.

Acknowledgments: This work was supported by the MPhil program "Advanced Technologies in Informatics and Computers", hosted by the Department of Computer Science, International Hellenic University, Greece.

Conflicts of Interest: The authors declare no conflict of interest.

References

1. Borenstein, J.; Everett, H.R.; Feng, L.; Wehe, D. Mobile robot positioning: Sensors and techniques. *J. Robot. Syst.* **1997**, *14*, 231–249. [CrossRef]
2. Kaplan, E.; Hegarty, C. *Understanding GPS: Principles and Applications*; Artech House: Norwood, MA, USA, 2005.
3. Lee, T.; Shin, J.; Cho, D. Position estimation for mobile robot using in-plane 3-axis IMU and active beacon. In Proceedings of the 2009 IEEE International Symposium on Industrial Electronics, Seoul, Korea, 5–8 July 2009; pp. 1956–1961.
4. King, A.D. Inertial navigation-forty years of evolution. *GEC Rev.* **1998**, *13*, 140–149.
5. You, Z. *Space Microsystems and Micro/Nano Satellites*; Butterworth-Heinemann: Beijing, China, 2017.
6. Kitchenham, B. Procedures for performing systematic reviews. *Keele UK Keele Univ.* **2004**, *33*, 1–26.
7. Khabsa, M.; Giles, C.L. The number of scholarly documents on the public web. *PLoS ONE* **2014**, *9*, e93949.
8. Hutter, M.; Gehring, C.; Jud, D.; Lauber, A.; Bellicoso, C.D.; Tsounis, V.; Hwangbo, J.; Bodie, K.; Fankhauser, P.; Bloesch, M.; et al. Anymal-a highly mobile and dynamic quadrupedal robot. In Proceedings of the 2016 IEEE/RSJ International Conference on Intelligent Robots and Systems (IROS), Daejeon, Korea, 9–14 October 2016; pp. 38–44.

9. Kim, W.; Lee, J.; Peternel, L.; Tsagarakis, N.; Ajoudani, A. Anticipatory robot assistance for the prevention of human static joint overloading in human–robot collaboration. *IEEE Robot. Autom. Lett.* **2017**, *3*, 68–75. [CrossRef]
10. Dubé, R.; Gawel, A.; Sommer, H.; Nieto, J.; Siegwart, R.; Cadena, C. An online multi-robot SLAM system for 3D LiDARs. In Proceedings of the 2017 IEEE/RSJ International Conference on Intelligent Robots and Systems (IROS), Vancouver, BC, Canada, 24–28 September 2017; pp. 1004–1011.
11. Yoon, P.K.; Zihajehzadeh, S.; Kang, B.; Park, E.J. Robust biomechanical model-based 3-D indoor localization and tracking method using UWB and IMU. *IEEE Sens. J.* **2016**, *17*, 1084–1096. [CrossRef]
12. Bartlett, H.L.; Goldfarb, M. A phase variable approach for IMU-based locomotion activity recognition. *IEEE Trans. Biomed. Eng.* **2017**, *65*, 1330–1338. [CrossRef]
13. Dang, Q.K.; Chee, Y.; Pham, D.D.; Suh, Y.S. A virtual blind cane using a line laser-based vision system and an inertial measurement unit. *Sensors* **2016**, *16*, 95. [CrossRef]
14. Meghdari, A.; Alemi, M.; Zakipour, M.; Kashanian, S.A. Design and realization of a sign language educational humanoid robot. *J. Intell. Robot. Syst.* **2019**, *95*, 3–17. [CrossRef]
15. Zhang, W.; Li, X.; Wei, D.; Ji, X.; Yuan, H. A foot-mounted pdr system based on imu/ekf+ hmm+ zupt+ zaru+ hdr+ compass algorithm. In Proceedings of the 2017 International conference on indoor positioning and indoor navigation (IPIN), Sapporo, Japan, 18–21 September 2017; pp. 1–5.
16. Li, B.; Ushiroda, K.; Yang, L.; Song, Q.; Xiao, J. Wall-climbing robot for non-destructive evaluation using impact-echo and metric learning SVM. *Int. J. Intell. Robot. Appl.* **2017**, *1*, 255–270. [CrossRef]
17. Wu, J.; Sun, L.; Jafari, R. A wearable system for recognizing American sign-language in real-time using IMU and surface EMG sensors. *IEEE J. Biomed. Health Inform.* **2016**, *20*, 1281–1290. [CrossRef] [PubMed]
18. Park, S.; Her, J.; Kim, J.; Lee, D. Design, modeling and control of omni-directional aerial robot. In Proceedings of the 2016 IEEE/RSJ International Conference on Intelligent Robots and Systems (IROS), Daejeon, Korea, 9–14 October 2016; pp. 1570–1575.
19. Alakshendra, V.; Chiddarwar, S.S. Adaptive robust control of Mecanum-wheeled mobile robot with uncertainties. *Nonlinear Dyn.* **2017**, *87*, 2147–2169. [CrossRef]
20. Liu, R.; Yuen, C.; Do, T.; Jiao, D.; Liu, X.; Tan, U. Cooperative relative positioning of mobile users by fusing IMU inertial and UWB ranging information. In Proceedings of the 2017 IEEE International Conference on Robotics and Automation (ICRA), Singapore, 29 May–3 June 2017; pp. 5623–5629.
21. Goldberg, B.; Zufferey, R.; Doshi, N.; Helbling, E.F.; Whittredge, G.; Kovac, M.; Wood, R.J. Power and control autonomy for high-speed locomotion with an insect-scale legged robot. *IEEE Robot. Autom. Lett.* **2018**, *3*, 987–993. [CrossRef]
22. Ando, H.; Ambe, Y.; Ishii, A.; Konyo, M.; Tadakuma, K.; Maruyama, S.; Tadokoro, S. Aerial hose type robot by water jet for fire fighting. *IEEE Robot. Autom. Lett.* **2018**, *3*, 1128–1135. [CrossRef]
23. Alcaide, J.O.; Pearson, L.; Rentschler, M.E. Design, modeling and control of a SMA-actuated biomimetic robot with novel functional skin. In Proceedings of the 2017 IEEE International Conference on Robotics and Automation (ICRA), Singapore, 29 May–3 June 2017; pp. 4338–4345.
24. Moore, T.; Stouch, D. A generalized extended kalman filter implementation for the robot operating system. In *Intelligent Autonomous Systems 13*; Springer: Berlin/Heidelberg, Germany, 2016; pp. 335–348.
25. Gregory, J.; Fink, J.; Stump, E.; Twigg, J.; Rogers, J.; Baran, D.; Fung, N.; Young, S. Application of multi-robot systems to disaster-relief scenarios with limited communication. In *Field and Service Robotics*; Springer: Berlin/Heidelberg, Germany, 2016; pp. 639–653.
26. Bjelonic, M.; Kottege, N.; Beckerle, P. Proprioceptive control of an over-actuated hexapod robot in unstructured terrain. In Proceedings of the 2016 IEEE/RSJ International Conference on Intelligent Robots and Systems (IROS), Daejeon, Korea, 9–14 October 2016; pp. 2042–2049.
27. Mangelson, J.G.; Dominic, D.; Eustice, R.M.; Vasudevan, R. Pairwise consistent measurement set maximization for robust multi-robot map merging. In Proceedings of the 2018 IEEE International Conference on Robotics and Automation (ICRA), Brisbane, Australia, 21–25 May 2018; pp. 2916–2923.
28. Song, Y.; Nuske, S.; Scherer, S. A multi-sensor fusion MAV state estimation from long-range stereo, IMU, GPS and barometric sensors. *Sensors* **2017**, *17*, 11. [CrossRef]
29. Bjelonic, M.; Kottege, N.; Homberger, T.; Borges, P.; Beckerle, P.; Chli, M. Weaver: Hexapod robot for autonomous navigation on unstructured terrain. *J. Field Robot.* **2018**, *35*, 1063–1079. [CrossRef]
30. Wang, W.; Mateos, L.A.; Park, S.; Leoni, P.; Gheneti, B.; Duarte, F.; Ratti, C.; Rus, D. Design, modeling, and nonlinear model predictive tracking control of a novel autonomous surface vehicle. In Proceedings of the 2018 IEEE International Conference on Robotics and Automation (ICRA), Brisbane, Australia, 21–25 May 2018; pp. 6189–6196.
31. Schwarz, M.; Rodehutskors, T.; Droeschel, D.; Beul, M.; Schreiber, M.; Araslanov, N.; Ivanov, I.; Lenz, C.; Razlaw, J.; Schüller, S.; et al. NimbRo Rescue: Solving disaster-response tasks with the mobile manipulation robot Momaro. *J. Field Robot.* **2017**, *34*, 400–425. [CrossRef]
32. Özaslan, T.; Loianno, G.; Keller, J.; Taylor, C.J.; Kumar, V.; Wozencraft, J.M.; Hood, T. Autonomous navigation and mapping for inspection of penstocks and tunnels with MAVs. *IEEE Robot. Autom. Lett.* **2017**, *2*, 1740–1747. [CrossRef]

33. Sampedro, C.; Rodriguez-Ramos, A.; Bavle, H.; Carrio, A.; de la Puente, P.; Campoy, P. A fully-autonomous aerial robot for search and rescue applications in indoor environments using learning-based techniques. *J. Intell. Robot. Syst.* **2019**, *95*, 601–627. [CrossRef]
34. Schwarz, M.; Rodehutskors, T.; Schreiber, M.; Behnke, S. Hybrid driving-stepping locomotion with the wheeled-legged robot Momaro. In Proceedings of the 2016 IEEE International Conference on Robotics and Automation (ICRA), Stockholm, Sweden, 16–21 May 2016; pp. 5589–5595.
35. Do, H.M.; Pham, M.; Sheng, W.; Yang, D.; Liu, M. RiSH: A robot-integrated smart home for elderly care. *Robot. Auton. Syst.* **2018**, *101*, 74–92. [CrossRef]
36. Ding, Y.; Galiana, I.; Siviy, C.; Panizzolo, F.A.; Walsh, C. IMU-based iterative control for hip extension assistance with a soft exosuit. In Proceedings of the 2016 IEEE International Conference on Robotics and Automation (ICRA), Stockholm, Sweden, 16–21 May 2016; pp. 3501–3508.
37. Gong, Y.; Hartley, R.; Da, X.; Hereid, A.; Harib, O.; Huang, J.K.; Grizzle, J. Feedback control of a cassie bipedal robot: Walking, standing, and riding a segway. In Proceedings of the 2019 American Control Conference (ACC), Philadelphia, PA, USA, 10–12 July 2019; pp. 4559–4566.
38. Klamt, T.; Rodriguez, D.; Schwarz, M.; Lenz, C.; Pavlichenko, D.; Droeschel, D.; Behnke, S. Supervised autonomous locomotion and manipulation for disaster response with a centaur-like robot. In Proceedings of the 2018 IEEE/RSJ International Conference on Intelligent Robots and Systems (IROS), Madrid, Spain, 1–5 October 2018; pp. 1–8.
39. Kundu, A.S.; Mazumder, O.; Lenka, P.K.; Bhaumik, S. Hand gesture recognition based omnidirectional wheelchair control using IMU and EMG sensors. *J. Intell. Robot. Syst.* **2018**, *91*, 529–541. [CrossRef]
40. Santos, F.N.D.; Sobreira, H.; Campos, D.; Morais, R.; Moreira, A.P.; Contente, O. Towards a reliable robot for steep slope vineyards monitoring. *J. Intell. Robot. Syst.* **2016**, *83*, 429–444. [CrossRef]
41. Parrott, C.; Dodd, T.J.; Groß, R. HyMod: A 3-DOF hybrid mobile and self-reconfigurable modular robot and its extensions. In *Distributed Autonomous Robotic Systems*; Springer: Berlin/Heidelberg, Germany, 2018; pp. 401–414.
42. Li, Y.; Guo, S.; Wang, Y. Design and characteristics evaluation of a novel spherical underwater robot. *Robot. Auton. Syst.* **2017**, *94*, 61–74. [CrossRef]
43. Koksal, N.; Jalalmaab, M.; Fidan, B. Adaptive linear quadratic attitude tracking control of a quadrotor UAV based on IMU sensor data fusion. *Sensors* **2019**, *19*, 46. [CrossRef] [PubMed]
44. Donthu, N.; Gustafsson, A. Effects of COVID-19 on business and research. *J. Bus. Res.* **2020**, *117*, 284–289. [CrossRef] [PubMed]